Appl. Phys. B 88, 545–549 (2007)
DOI: 10.1007/s00340-007-2722-7

Applied Physics B
Lasers and Optics

G. ZHENG
W. SHE✉

Fast and wide-range continuously tunable Šolc-type filter based on periodically poled $LiNbO_3$

State Key Laboratory of Optoelectronic Materials and Technologies, Sun Yat-Sen University, Guangzhou 510275, P.R. China

Received: 28 March 2007/Revised version: 1 June 2007
Published online: 7 July 2007 •

ABSTRACT We present a fast and wide-range continuously tunable Šolc-type filter based on periodically poled $LiNbO_3$ (PPLN) in this paper. The filter is formed in PPLN by applying a biased dc electric field along the y-axis, and the tuning of a transmitted central wavelength is realized by applying another dc electric field along the z-axis. The numerical results demonstrate that the tuning range covers as much as 16 nm, and the dependence of the transmitted central wavelength shift on the control electric field, shows a nearly linear relation with a tuning rate of 0.95 kV/mm per nm.

PACS 42.65.-k; 78.20.Jq; 42.79.Ci

1 Introduction

In recent years, PPLN has attracted more and more research attention because of its outstanding nonlinear optical properties, and a number of interesting results have been found [1–4]. The quasi-phase-matching (QPM), based on the periodic variation of the sign of the nonlinear optical coefficient, has become a very useful technology to match a nonlinear process in phase efficiently [5]. Besides the nonlinear optical coefficients relative to the second-order parametric processes, the EO coefficients are also periodically modulated because of periodically reversed ferroelectric domains in PPLN. Therefore, the concept of QPM is also valid in the linear electro-optic effect, and some interesting phenomena have been observed [6–8]. Similar to that in the nonlinear optical frequency conversion process, the reciprocal vector of the periodic structure can be used to compensate the phase mismatch between the o- and e-rays for the electro-optic effect. Lu et al. theoretically predicted that a precise spectral filter can be realized in PPLN by applying a uniform dc electric field along the y-axis [6]. Later, Chen et al. experimentally demonstrated a Šolc-type filter in PPLN with and without a uniform dc electric field along the y-axis [9–12]. They tuned the transmitted central wavelength thermally or by UV-light illumination [9–12]. Compared to a traditional Šolc-type filter [13], the PPLN EO Šolc-type filter can be realized in one chip of lithium niobate, and the output intensity of the filter can be controlled electrically, which leads to simultaneous achievements of a modulator and a filter in one piece of PPLN [11]. Instead of calefaction or UV-light illumination, we find that under certain conditions the tuning of the transmitted central wavelength can be achieved by applying a dc electric field along the z-axis of the PPLN with a biased one along the y-axis. Since the tuning is based on the linear electro-optic effect, it would have a much faster response than those of thermal and UV-illumination types. As the QPM condition is very sensitive to the wavelength and the largest electro-optic coefficient is utilized, the filter has a narrowband spectrum and a broad tuning range (above 16 nm). The dependence of the transmitted central wavelength shift on the control electric field shows a nearly linear relation with a tuning rate of 0.95 kV/mm per nm. In the following, we will discuss this kind of filter in detail.

✉ Fax: +86-20-84037423, E-mail: shewl@mail.sysu.edu.cn

2 Theory and calculation

In our previous work, we have generalized the wave coupling theory of the linear electro-optic effect [14] to the case of QPM materials [15]. For the case in which only a single QPM order is valid and all other orders are off phase matching, the coupling equations describing the QPM linear electro-optic effect have been obtained as follows [15]

$$\frac{\mathrm{d}A_1(r)}{\mathrm{d}r} \approx -\mathrm{i}\kappa_q A_2(r)\exp(\mathrm{i}\Delta k r) - \mathrm{i}\upsilon_{1q}A_1(r)\,, \tag{1a}$$

$$\frac{\mathrm{d}A_2(r)}{\mathrm{d}r} \approx -\mathrm{i}\kappa_q^* A_1(r)\exp(-\mathrm{i}\Delta k r) - \mathrm{i}\upsilon_{2q}A_2(r)\,, \tag{1b}$$

with

$$\Delta k = k_2 - k_1 + \alpha_m\,, \quad \alpha_m = \frac{2m\pi}{\Lambda}\,,$$

$$\kappa_q = \frac{k_0}{2\sqrt{n_1 n_2}} r_{\mathrm{eff1}} E_0 G_m\,, \quad \kappa_q^* = \frac{k_0}{2\sqrt{n_1 n_2}} r_{\mathrm{eff1}} E_0 G_{-m}\,,$$

$$\upsilon_{1q} = \frac{k_0}{2n_1} r_{\mathrm{eff2}} E_0 G_0\,, \quad \upsilon_{2q} = \frac{k_0}{2n_2} r_{\mathrm{eff3}} E_0 G_0\,,$$

$$G_m = \frac{1}{\mathrm{i}\pi m}[1-\cos(2\pi m D) + \mathrm{i}\sin(2\pi m D)] \quad (m \neq 0)\,,$$

$$G_0 = 2D - 1\,,$$

where $A_1(r)$ and $A_2(r)$ are the normalized amplitudes of two independent components of the light field; n_1, n_2 and k_1, k_2 are the corresponding unperturbed refractive indices and wave numbers; k_0 is the wave number of light in vacuum; α_m is the amplitude of the m-th reciprocal vector, Λ is the poling period, D is duty cycle of the structure defined by $D = l/\Lambda$ and l is the length of one positive section; E_0 is the amplitude of the external electric field; $r_{\mathrm{eff}i}$ ($i = 1,2,3$) are the effective electro-optic coefficients [14]. In particular, G_0 is zero when the duty cycle D is 0.5, which leads to $v_{1q} = v_{2q} = 0$. In this case, the resultant equations are reduced to those of coupled-mode theory where the terms v_{1q} and v_{2q} disappear [16], which should be avoided because $v_{1q} - v_{2q}$ is just the variable controlling the transmitted central wavelength in our method.

Assuming the incident light is an e-ray propagating along the x-axis with the initial condition $A_1(0) = 0$, $A_2(0) = 1$, the solution of the (1) can be easily obtained:

$$A_1(r) = -\mathrm{i}\exp(\mathrm{i}\beta r)\frac{\kappa_q}{\mu}\sin(\mu r)\,, \tag{2}$$

$$A_2(r) = \exp[\mathrm{i}(\beta - \Delta k)r]\left[\cos(\mu r) - \mathrm{i}\frac{\gamma}{\mu}\sin(\mu r)\right], \tag{3}$$

where

$$\mu = \frac{1}{2}\sqrt{(\Delta k + v_{1q} - v_{2q})^2 + 4\kappa_q\kappa_q^*}\,, \tag{4}$$

$$\gamma = \frac{1}{2}(v_{2q} - v_{1q} - \Delta k)\,, \quad \beta = \frac{1}{2}(\Delta k - v_{1q} - v_{2q})\,. \tag{5}$$

The output intensity of the o-ray I_o is thus given by

$$I_\mathrm{o} = \frac{|\kappa_q|^2}{\mu^2}\sin^2(\mu L)\,, \tag{6}$$

where L is the effective length of the crystal. From (4) and (6), one can see that the output intensity of the o-ray depends not only on the QPM condition (Δk) but also on the value of $v_{2q} - v_{1q}$. And the maximal conversion efficiency occurs at

$$\Delta k + v_{1q} - v_{2q} = 0\,, \tag{7}$$

and

$$\sin(|\kappa|L) = 1\,. \tag{8}$$

Since relation (7) is very sensitive to the wavelength, the output intensity of the o-ray decreases remarkably if the wavelength shifts a little [15]. This is the reason why it can act as a filter.

Figure 1 shows the basic schematic diagram of an electrically tunable PPLN filter. The filter consists of a 2.5 cm z-cut PPLN placed between two cross polarizers, in which the polarization direction of the front one is set parallel to z-axis and the other parallel to y-axis of the PPLN. The duty cycle of the PPLN used here is 0.75, i.e., the ratio of the neighbouring positive- and negative-domain widths is 3 : 1, which is the optimum value of second-order quasi-phase matching [15]. The poling period is $\Lambda = 2\lambda_0/[n_o(\lambda_0) - n_e(\lambda_0)]$ ($\lambda_0 = 1550$ nm), which means that the second-order ($m = 2$) QPM condition is satisfied for light with $\lambda_0 = 1550$ nm, propagating along the x-axis.

In the literature, the duty cycle of PPLN chosen was $D = 0.5$ [6, 9–12], and the electric field used was only along the y-axis [6, 11]. In our design, two electric fields are used, one of which is along the y-axis and another is along the z-axis. The total external electric field is thus

$$\boldsymbol{E}(0) = E_0\,\boldsymbol{c} = E_0\left(\frac{E_y}{E_0}\boldsymbol{j} + \frac{E_z}{E_0}\boldsymbol{k}\right), \tag{9}$$

where $\boldsymbol{c}$ is the unit vector of $\boldsymbol{E}(0)$; E_y and E_z are the amplitudes of external electric fields along the y-axis and z-axis; $E_0 = \sqrt{E_y^2 + E_z^2}$; and $\boldsymbol{j}$ and $\boldsymbol{k}$ are the two corresponding unit vectors pointing to positive directions of y-axis and z-axis. When E_y and (or) E_z change, both the direction and amplitude of the total external filed will change. For a regular $LiNbO_3$, the contracted form of the crystal-frame (xyz) expression of the electro-optic tensor is

$$\tilde{r} = \begin{pmatrix} 0 & -r_{22} & r_{23} \\ 0 & r_{22} & r_{23} \\ 0 & 0 & r_{33} \\ 0 & r_{51} & 0 \\ r_{51} & 0 & 0 \\ -r_{22} & 0 & 0 \end{pmatrix}, \tag{10}$$

where the four independent electro-optic coefficients are $r_{22} = 3.4$, $r_{23} = 8.6$, $r_{33} = 30.8$, and $r_{51} = 28$ (in 10^{-12} m/V) [14]. Therefore, in the presence of the external electric field $\boldsymbol{E}(0)$, we have

$$\kappa_q = -\mathrm{i}\frac{n_0^2 n_e^2}{2\pi\sqrt{n_o n_e}}k_0 r_{51}E_y\,, \quad \kappa_q^* = \mathrm{i}\frac{n_0^2 n_e^2}{2\pi\sqrt{n_o n_e}}k_0 r_{51}E_y\,, \tag{11}$$

and

$$v_{2q} - v_{1q} = -\frac{1}{4}n_o^3 r_{22}k_0E_y + \frac{1}{4}(n_e^3 r_{33} - n_o^3 r_{23})k_0E_z\,. \tag{12}$$

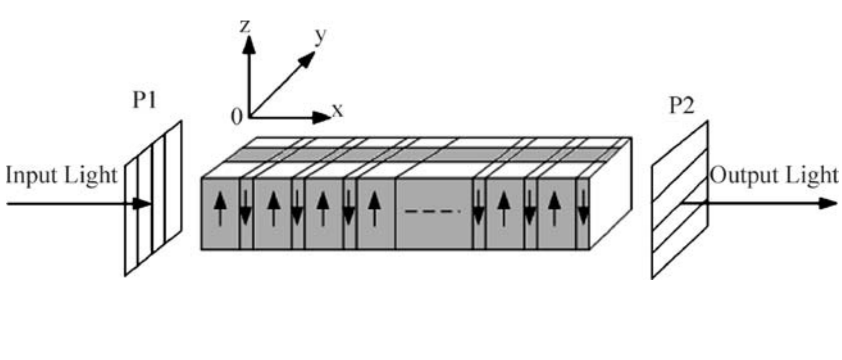

FIGURE 1 The basic schematic diagram of the EO PPLN Šolc-type filter

It should be emphasized that the nonzero $\upsilon_{2q}-\upsilon_{1q}$ appears only when the duty cycle is not equal to 0.5. Equation (11) clearly shows that $\kappa_q(\kappa_q^*)$ is independent of E_z, and it is controlled by E_y. However, the value of $\upsilon_{2q}-\upsilon_{1q}$ depends strongly on E_z through the largest electro-optic coefficient r_{33}. Since the refractive indexes are the functions of wavelength, relation (7) reads

$$[n_e(\lambda)-n_o(\lambda)]\frac{1}{\lambda}+\frac{2}{\Lambda}+\frac{n_o^3(\lambda)}{4\lambda}r_{22}E_y - \frac{1}{4\lambda}\left[n_e^3(\lambda)r_{33}-n_o^3(\lambda)r_{23}\right]E_z=0\,. \tag{13}$$

From (13), one can see that the transmitted central wavelength will shift when E_z is applied. For a fixed electric field E_y, the output intensity of the filter almost stays unchanged although the wavelength shifts by tens of nanometers, because $\sin(|\kappa|L)$ is insensitive to the wavelength. But, the output intensity of the filter can be controlled by varying the electric field E_y, which is reflected by $\sin(|\kappa|L)$.

In order to find the optimum condition for the output intensity of the filter, we first study the relation between the output intensity of the o-ray (or the e-ray) and E_y. For numerical simulations, the Sellmeier equations for $LiNbO_3$ are necessary, which are [17]

$$\begin{aligned} n_o^2 &= 4.9130+\frac{1.173\times10^5+1.65\times10^{-2}T^2}{\lambda^2-(2.12\times10^2+2.7\times10^{-5}T^2)^2} \\ &\quad -2.78\times10^{-8}\lambda^2\,, \\ n_e^2 &= 4.5567+2.605\times10^{-7}T^2 \\ &\quad +\frac{0.970\times10^5+2.70\times10^{-2}T^2}{\lambda^2-(2.01\times10^2+5.4\times10^{-5}T^2)^2} \\ &\quad -2.24\times10^{-8}\lambda^2\,, \end{aligned} \tag{14}$$

where T is the absolute temperature and λ is the wavelength of incident light in nm. The results shown in Fig. 2 are obtained under the conditions of $\lambda_0 = 1550$ nm and $T = 298$ K (25 °C) when E_z is absent. One can see that about 99% energy of the e-ray is transferred to the o-ray when the external field E_y is 0.33 kV/mm. The conversion efficiency cannot reach 100% since the duty cycle is not 0.5. In fact, a much higher extinction ration for the 0.75 duty cycle can be achieved by adding a variable retarder [19].

So, we fix the external electric field E_y at 0.33 kV/mm and study the dependence of the output intensity of the o-ray on the wavelength of the light. Figure 3 shows the results corresponding to $E_z = 0$ and $E_z = \pm1.9$ kV/mm, respectively. One can see that the transmitted central wavelength shifts as much as 2 nm when $E_z = \pm1.9$ kV/mm. The full width at half maximum (FWHM) of the filter is about 1 nm, which can even be narrowed to 0.5 nm if the length of the PPLN is doubled. In fact, the FWHM is inversely proportional to the crystal length, so a much narrower spectrum filter then expected can be achieved by the employment of a long enough PPLN crystal. The relation between the transmitted central wavelength and the control electric field E_z would be useful for practical applications. The numerical result is shown in Fig. 4, in which the dependence of the transmitted central wavelength on the control electric field E_z shows a nearly linear relation with a tuning rate of about 0.95 kV/mm per nm. The stronger the control electric field E_z, the larger the shift of the transmitted central wavelength is. However, for an undoped PPLN the electrical breakdown limits the electric field to a maximum value of 16.8 kV/mm [18]. In our calculations, the electric field E_z is set in a safe region from −7.6 kV/mm to 7.6 kV/mm, which gives the transmitted central wavelength from 1558 nm to 1542 nm.

Now we discuss how the filter works in a well known manner. In our design, the coherence length [6], i.e., $L_c = \lambda_0/2(n_o-n_e)$, is 10.26 μm, which is achievable for current fabrication techniques. For the case of $D = 0.75$ used in our design, every poling period Λ consists of a $3L_c$ long positive domain and a L_c long negative one, so both the positive and negative domains act as a half-wave plate. For regular $LiNbO_3$ with an external field E_y, the field-modified index tensor becomes [19]

$$\eta=\begin{pmatrix} \frac{1}{n_o^2}-r_{22}E_y & 0 & 0 \\ 0 & \frac{1}{n_o^2}+r_{22}E_y & r_{51}E_y \\ 0 & r_{51}E_y & \frac{1}{n_e^2} \end{pmatrix}\,, \tag{15}$$

and the new index ellipsoid is given by

$$\left(\frac{1}{n_o^2}-r_{22}E_y\right)x^2+\left(\frac{1}{n_o^2}+r_{22}E_y\right)y^2+\frac{1}{n_e^2}z^2+2r_{51}E_yyz = 1\,. \tag{16}$$

Hence, the new index ellipsoid deforms, which makes the y- and z-axis rotate by a small angle $\theta \approx r_{51}E_y/(1/n_e^2-1/n_o^2)$ around the x-axis [6]. The azimuth angle of the new z-axis thus rocks right and left from θ to $-\theta$ due to the periodic EO coefficient in PPLN. Therefore, a folded Šolc-type filter is formed by a uniform electric field along the y-axis. However, when the external electric field E_z is introduced, the directions of each of the three axis of the new index ellipsoid remain unchanged since no mixed terms appear [13]. The new principle

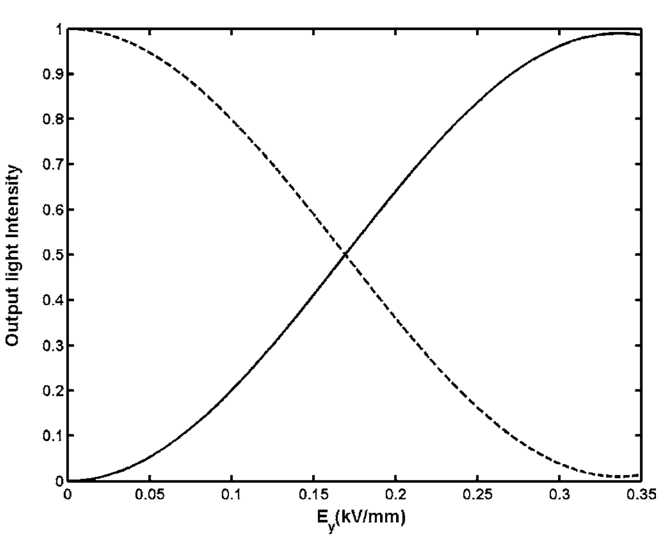

FIGURE 2 The output intensity of o-ray (*solid line*) or e-ray (*dashed line*) as a function of the external electric field E_y with an absence of E_z

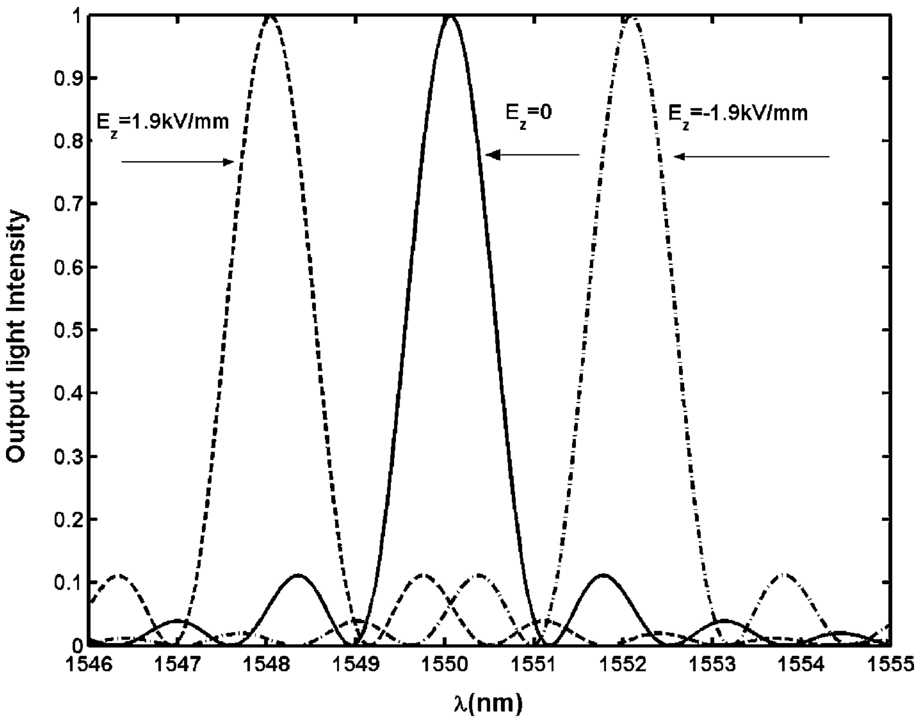

FIGURE 3 The output intensity of the EO PPLN Šolc-type filter as a function of wavelength λ. The *solid line*, *dashed line* and *dashed-dot line* correspond to $E_z = 0\,\mathrm{kV/mm}$, $E_z = 1.9\,\mathrm{kV/mm}$ and $E_z = -1.9\,\mathrm{kV/mm}$, respectively

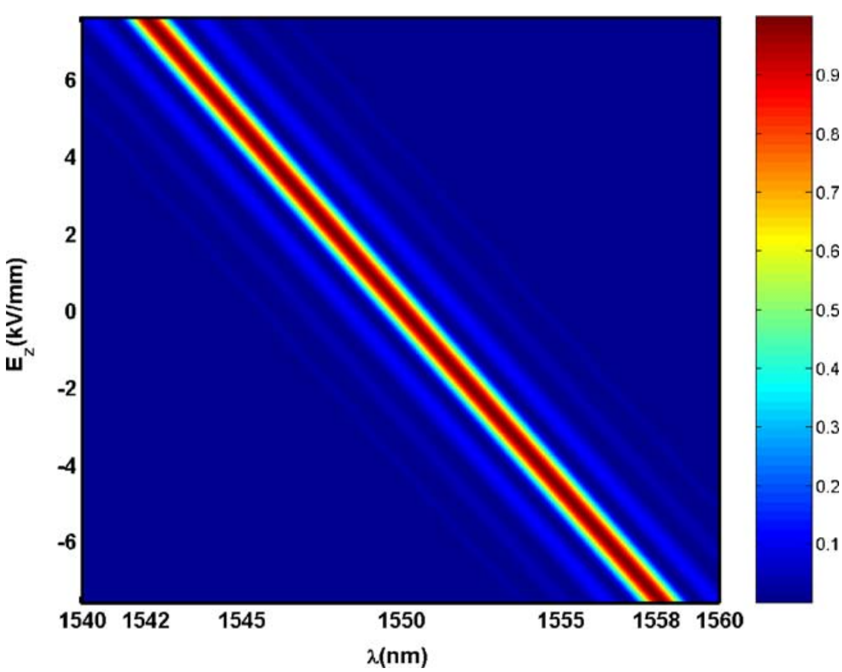

FIGURE 4 The output intensity of the EO PPLN Šolc-type filter as a function of the control field E_z and the incident light wavelength λ

refractive indices change as [13]

$$n_x{}' = n_y' = n_o\left(1 + n_o^2 r_{23} E_z\right)^{-0.5} \approx n_o - \frac{1}{2} n_o^3 r_{23} E_z\,, \tag{17}$$

$$n_z' = n_e\left(1 + n_e^2 r_{33} E_z\right)^{-0.5} \approx n_e - \frac{1}{2} n_e^3 r_{33} E_z\,. \tag{18}$$

Therefore, the equivalent birefringence of the PPLN with E_z, seen by a light beam propagating along the x-axis of the PPLN, becomes

$$n_z - n_y = (n_e - n_o) - \frac{1}{2}(2D-1)\left(n_e^3 r_{33} - n_o^3 r_{23}\right) E_z\,. \tag{19}$$

So the transmitted central wavelength will shift if E_z is applied except for $D = 0.5$, since there is no electro-optical birefringence induced when $D = 0.5$.

3 Conclusion

We have demonstrated a fast wide-range tunable PPLN Šolc-type filter with a biased dc electric field along the y-axis, for which the central wavelength can be tuned by varying the electric field along the z-axis. Thanks to the sensitivity of the tuning, the tuning range can cover above 16 nm with a tuning rate of 0.95 kV/mm per nm.

ACKNOWLEDGEMENTS This work is supported by the National Natural Science Foundation of China (Grant No. 10574167).

REFERENCES

1 G.A. Magel, M.M. Fejer, R.L. Byer, Appl. Phys. Lett. **56**, 108 (1990)
2 D.H. Jundt, G.A. Magel, M.M. Fejer, R.L. Byer, Appl. Phys. Lett. **59**, 2657 (1991)
3 J.J. Zheng, Y.Q. Lu, G.P. Luo, J. Ma, Y.L. Lu, N.B. Ming, J.L. He, Z.Y. Xu, Appl. Phys. Lett. **72**, 1808 (1998)
4 Y.Q. Lu, J.J. Zheng, Y.L. Lu, N.B. Ming, Appl. Phys. Lett. **74**, 123 (1999)
5 M.M. Fejer, G.A. Magel, D.H. Jundt, R.L. Byer, IEEE J. Quantum Electron. **QE-28**, 2631 (1992)
6 Y.Q. Lu, Z.L. Wan, Q. Wang, Y.X. Xi, N.B. Ming, Appl. Phys. Lett. **77**, 3719 (2000)
7 Y.Q. Lu, M. Xiao, G.J. Salamo, Appl. Phys. Lett. **78**, 1035 (2001)
8 J.H. Shi, X.F. Chen, Y.X. Xia, Y.L. Chen, Appl. Opt. **42**, 5722 (2003)
9 J.H. Shi, J.H. Wang, L.J. Chen, X.F. Chen, Y.X. Xia, Opt. Express **14**, 6279 (2006)
10 L.J. Chen, J.H. Shi, X.F. Chen, Y.X. Xia, Appl. Phys. Lett. **88**, 121 118 (2006)
11 X.F. Chen, J.H. Shi, Y.P. Chen, Y.M. Zhu, Y.X. Xia, Y.L. Chen, Opt. Lett. **28**, 2115 (2003)
12 Y.M. Zhu, X.F. Chen, J.H. Shi, Y.P. Chen, Y.X. Xia, Y.L. Chen, Opt. Commun. **228**, 139 (2003)
13 A. Yariv, P. Yeh, *Optical Waves in Crystal: Propagation and Control of Laser Radiation* (Wiley, New York, 1984)
14 W.L. She, W.K. Lee, Opt. Commun. **195**, 303 (2001)
15 G.L. Zheng, H.C. Wang, W.L. She, Opt. Express **14**, 5535 (2006)
16 A. Yariv, IEEE J. Quantum Electron. **QE-9**, 919 (1973)
17 M.V. Hobden, J. Warner, Phys. Lett. **22**, 243 (1966)
18 Q.X. Xi, D.A. Liu, Y.N. Zhi, Z. Luan, L.R. Liu, Appl. Phys. Lett. **87**, 121 103 (2005)
19 E. Rabia, A. Arie, Appl. Opt. **45**, 540 (2006)